A Status Review of Failure Simulation at the Federal Aviation Administration

Daniel Cordasco[1], William Emmerling[1], Paul Du Bois[2]

[1]Federal Aviation Administration
William J. Hughes Technical Center
Atlantic City Int'l Airport 08405

[2]Consulting Engineer, Northville, MI

1 Abstract

The Federal Aviation Administration (FAA) is developing models and methods for simulating fan blade-off impact for engine containment. Accurately predicting deformation and failure in such an event is essential for advancing the industry and FAA goal of certification by analysis. Furthermore, industry and government engineers require publicly available tools to standardize the analysis during the engine design, development, and certification phase. In addition to the high strain rates and steep temperature gradients typically realized in the impact event, a complex 3-D state of stress develops, which is dependent on the impactor and target material properties, geometry, relative orientation, and impact velocity. The resulting failure surfaces which characterize the plastic failure strain by the state of stress fully defined by the triaxiality and Lode parameter are highly nonlinear. Often, crucial stress-state data points are not easily realized by typical specimen-level standard tests necessitating the development of new experiments to fully characterize the surface for a given material.

The FAA Aircraft Catastrophic Failure Prevention Program (ACFPP), working in conjunction with government, academia, and industry, has made considerable progress in developing a family of tabulated plasticity models based on the Johnson-Cook (J-C) approach available in LS-DYNA (MAT_224, MAT_224_GYS, and MAT_264). These models have been created to meet the particular need for simulations that can predict the transition from petaling to plugging failure modes as well as the intermediate mixed modes that develop with changing target plate thickness and impact speed. In addition, the material constitutive and failure response for several typical aerospace metals, including Ti-6Al-4V, Al-2024, Inconel-718, and stainless steel 410, is underway. During testing, it was observed that a tensile-compressive asymmetry in yield and an anisotropic directional dependence may arise for some materials depending on inherent material microstructure and also the manufactured plate thickness. Therefore, each model offers an increasing degree of capability in modeling these phenomena. These tasks have highlighted some of the challenges in complex failure modeling and underscore the need for a robust experimental testing program to complement computational modeling.

2 Background

The FAA ACFPP has sponsored research since the mid-1990s aimed at addressing the design issues encountered during the certification process with the goal of minimizing the hazard to the aircraft from uncontained engine debris. This requirement is defined in Title 14 of the Code of Federal Regulations (CFR) 25.903, and methods of compliance are set forth in Advisory Circular AC 20-128A. The impact analysis problem encountered in satisfying this requirement is very similar to the analysis for certification of engine fan blade-out containment. Title 14 CFR 33.94 states, "it must be demonstrated by engine tests that the engine is capable of containing damage without catching fire and without failure of its mounting attachments when operated for at least 15 seconds, …Failure of the most critical compressor or fan blade while operating at maximum permissible r.p.m. …". Analysis can only be used to supplement compliance by test under certain circumstances on a case-by-case basis and always must be backed up by a validation study.

The FAA ACFPP has worked closely with the National Aeronautics and Space Administration–Glenn Research Center's (NASA–GRC) Impact Dynamics Group over the years and partnered with academia and industry through the LS-DYNA Aerospace Working Group (AWG) to develop impact test data and analytical capabilities that have advanced the state of the art used in modeling metal, composite, and impact-resistant fabrics for aerospace vehicle safety. A primary goal has been to develop a physics-based analysis approach that can accurately predict the mode of failure and

damage from a turbine engine fragment impact to the engine or aircraft structure. Modeling impact of metallic materials has been a primary thrust of the research and is the subject of this review paper.

This research stems from an event which occurred in 1989, when a McDonnell Douglas DC-10 experienced an uncontained engine failure while in cruise flight that disabled the triple-redundant flight control systems severely affecting the controllability of the aircraft. The flight crew was able to use differential engine power to crudely control the plane to a crash landing at Sioux City International Airport, South Dakota. Of the 296 passengers and crew onboard, there were 111 fatalities. The United States Congress subsequently established the FAA ACFPP in 1990 (Public Law 101-508) with the purpose of improving aircraft system safety.

The FAA ACFPP program has focused on uncontained engine failure modeling and mitigation as a primary area of research since its inception. Additional related research areas include aircraft vulnerability analysis from an uncontained event and developing lightweight protection systems for shielding from engine fragments. In 2002, an Airworthiness Assurance Center of Excellence was established by the FAA which provided funding with an equal cost match from industry. A team composed of University of California at Berkeley (UCB) partnered with Lawrence Livermore National Laboratory and The Boeing Company to continue work on metallic impact failures. Testing of fragment barrier systems provided detailed ballistic impact response data for different thickness aluminum plates (as well as polycarbonate and sandwich composites) which could be used to evaluate modeling capability [1]. Further modeling of impact events using the J-C model found that the material parameters could be tuned to match test data quite accurately. However, the model parameters needed to be adjusted to elicit a specific mode of failure such that the failure mode had to be known before an accurate analysis could be performed [2]. Therefore, this approach of adjusting J-C material parameters to match each failure mode could not be considered truly predictive particularly when considering a large-scale simulation with complex geometries, a large range of velocities, and varying target thickness. As the aviation industry and FAA pursue greater use of certification by analysis for such requirements as the fan blade-out test defined in 14 CFR 33.94, predictive accuracy is essential. This need has been met by FAA investment in developing advanced material models in LS-DYNA capable of accurately predicting metallic deformation and failure during an impact event.

3 Research Products

A primary objective of the ACFPP has been to improve the analytical capability of modeling engine fragments impacting the engine case as in the fan blade-out containment requirement Title 14 CFR 33.94 and also in rare cases in which fragments exit the case. This problem necessitates accurate modeling of the nonlinear plastic region of the stress-strain curve all the way up to and including the rupture point of the material. The task is complicated by the wide range of fragment velocities that can vary from as low as 200 ft/s up to 900 ft/s, which fall between two well-studied impact events of automobile crash and blast penetration. The broad range of speed along with the varying target thicknesses and projectile shapes and orientations creates a unique problem necessitating a model that can predict multiple failures with a single set of input material properties. Evaluating the survivability of aircraft systems also requires an accurate assessment of energy absorbed and the residual velocity after penetration.

The FAA ACPP set about this effort by conducting initial tests characterizing the material properties and ballistic limits on aerospace metallic alloys. Empirical constants were fit to the experimental ballistic test data, and it eventually became apparent that the failure could be modeled using the J-C approach for a given plate thickness to correlate well with test results. However, changing the thickness, velocity, or projectile shape could alter the failure mode, which would require tuning the model to a new set of constants to closely match the experimental data. This is shown in figure 1.

The need to tune the J-C model for a particular failure mode precludes its use as a predictive model that can be used for certification by analysis. As a result, the FAA ACFPP research program has pursued development of several new material models incorporated into LS-DYNA for metal failure, namely MAT_224, MAT_224_GYS, and MAT_264. This research effort has been active for many years, and the progress has been a result of a combination of advancing technology and a better understanding of metallic failure from considerable testing and simulation efforts. All models are based on the concept of creating tabulated curves for the material law tabulating plastic failure strain as a function of the state of stress. In addition, all models have the ability to consider the plastic response and failure strains as dependent on temperature and strain rate. An accompanying extensive

experimental testing program has provided the material characterization test data for the models. A brief overview of the model features are given in this section. The current and future program emphasis is placed on rigorous validation of the models against ballistic impact test data for several aerospace metals.

Fig.1: Failure mode transition from petaling to plugging with target thickness and projectile energy.

3.1 Initial Assessment with MAT_15 Johnson-Cook

The Johnson-Cook (J-C) model is one of the most commonly used material models for dynamic impact applications [3]. The FAA began by evaluating the ability of the J-C model in LS-DYNA to represent the deformation and failure response of 2024-T3 aluminum plate with three different thicknesses of 0.0625″, 0.125″, and 0.25″ [1, 2]. The ballistic impact test data was conducted by UCB using a 0.5″ spherical steel projectile fired by gas and powder guns against flat 12″ by 12″ plates to attain the ballistic limit and residual velocities after penetration. Ductile failure was observed in which the aluminum plates failed by dishing and petaling with slight plugging for the 0.0625″ targets. The petaling failure morphology is characterized by significant bending deformation and radial tearing of the impact zone into petal-like shapes. As the thickness was increased, the relative amount of petaling decreased and the failure transitioned to a plugging-dominated mode. The plugging failure shows little deformation in the impact zone and a straight-sided coin-like plug is generated (see figure 1).

The J-C material law assumes that the flow stress of the material can be related to a multiplicative decomposition of strain hardening, strain-rate hardening, and thermal softening. The strength is assumed to be isotropic and independent of the mean stress (J_2 flow theory). The flow stress is expressed as

$$\sigma_y = \left[A + B\varepsilon_p^n\right]\left[1 + C\ln\dot{\varepsilon}^*\right]\left[1 - \left(\frac{T - T_R}{T_m - T_R}\right)^m\right] \tag{1}$$

where σ is the yield stress; ε_p is the effective plastic strain; $\dot{\varepsilon}^* = \dot{\varepsilon}/\dot{\varepsilon}_0$ is the normalized effective plastic strain rate; n is the work hardening exponent; *A*, *B*, *C*, and *m* are constants; T_R is the ambient temperature; and T_{melt} is the melting temperature.

The values of the constants *A*, *B*, *C*, and *m* are determined from an empirical fit of flow stress data from experiment to equation (1). Failure is modeled using a cumulative damage law in which failure occurs when the damage, *D*, reaches 1:

$$D = \sum \frac{\Delta\varepsilon_p}{\varepsilon_{pf}} \tag{2}$$

where $\Delta\varepsilon_p$ is the increment of effective plastic strain and the plastic failure strain ε_{pf} is a function of stress triaxiality, strain rate, and temperature defined as

$$\varepsilon_{pf} = \left[D_1 + D_2 \exp\left(D_3\sigma^*\right)\right]\left[1 + D_4 \ln\dot{\varepsilon}^*\right]\left[1 - D_5\left(\frac{T - T_R}{T_m - T_R}\right)^{*m}\right] \tag{3}$$

where the parameters D_1, D_2, D_3, D_4, D_5 are constants. The state of stress is expressed by the stress triaxiality σ^* defined as

$$\sigma^* = \frac{p}{\sigma_{vm}} \tag{4}$$

where p is the pressure and σ_{vm} is the von Mises stress, which is related to the second invariant J_2 of the deviatoric stress tensor $\sigma_{vm} = \sqrt{3J_2}$. The triaxiality can vary between $-\infty < \sigma^* < \infty$ with the lower and upper limits corresponding to hydrostatic tension and compression.

The primary motivation for further research pursuing development of improved material models for impact is exemplified in figure 2. Figure 2 shows the simulation results using the J-C model in LS-DYNA with a parameter set of material constants tuned to match failure data for the 0.125″ plate applied to all three plate thicknesses. As illustrated, the simulations match the 0.125″ test data to which the model data was tuned, but they overpredict the ballistic limit for 0.0625″ and underpredict the ballistic limit for 0.250″. It was not possible to accurately match to the test data from all three thicknesses with a single set of material constant using the J-C model.
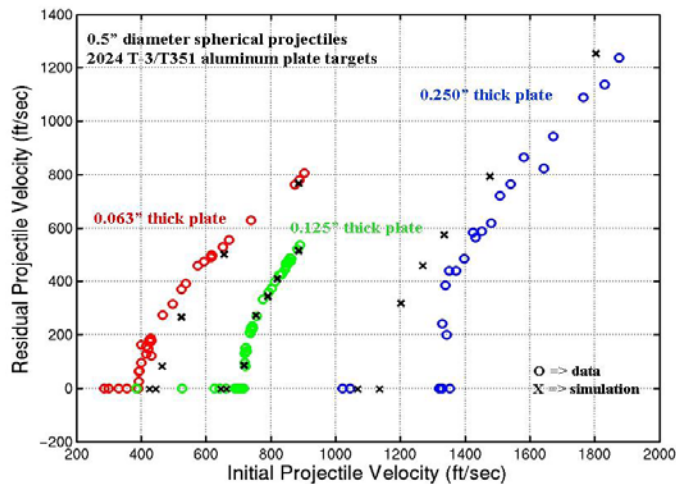
Fig.2: *Ballistic test data vs. MAT_15 simulations tuned for material parameter to match the 0.125″-thick plate [2].*

3.2 Development of MAT_224 *MAT_TABULATED_JOHNSON_COOK

To accomplish the FAA objective of prediction accuracy over a range of failure modes, several features were identified which could improve representation of the deformation and failure physics. This development work has resulted in a new material model available in LS-DYNA, MAT_224 given the full keyword *MAT_TABULATED_JOHNSON_COOK.

The petaling and plugging failure modes, as well as the intermediate mixed mode, occupy different states of stress and therefore will have different triaxialities. Figure 3 shows the failure plastic strain for two sets of MAT_15 J-C parameters tuned for petaling and plugging failures. The petaling failure occurs at a higher plastic strain than plugging. Because of the monotonic nature of the exponential dependence of plastic failure strain on triaxiality in the J-C model, it can be tuned to match the petaling or plugging failure, but not both. However, adopting an approach in which the failure plastic strain

dependence on triaxiality is expressed in a tabulated form, MAT_224 can capture both failure modes and the transition between them based on a set of actual material test data.

Mesh regularization, in which the element erosion dependency on element size is mitigated, was identified early on as a necessary feature. The team also concluded that the plastic strain accumulation and failure should be a function of the full 3-D state of stress. This required the consideration of the Lode parameter θ_L in addition to triaxiality to fully define the 3-D state of stress.

$$\theta_L = \frac{27 J_3}{2\sigma_{vm}^3} \tag{5}$$

where J_3 is the third deviatoric stress invariant. The Lode parameter can vary between $-1 < \theta_L < 1$, with the lower and upper limits corresponding to compressive and tensile axisymmetric states of stress. Therefore, the 2-D failure curves presented in figure 3 became a 3-D failure surface (e.g., figure 4) in which failure plastic strain is dependent on both triaxiality and Lode parameter.
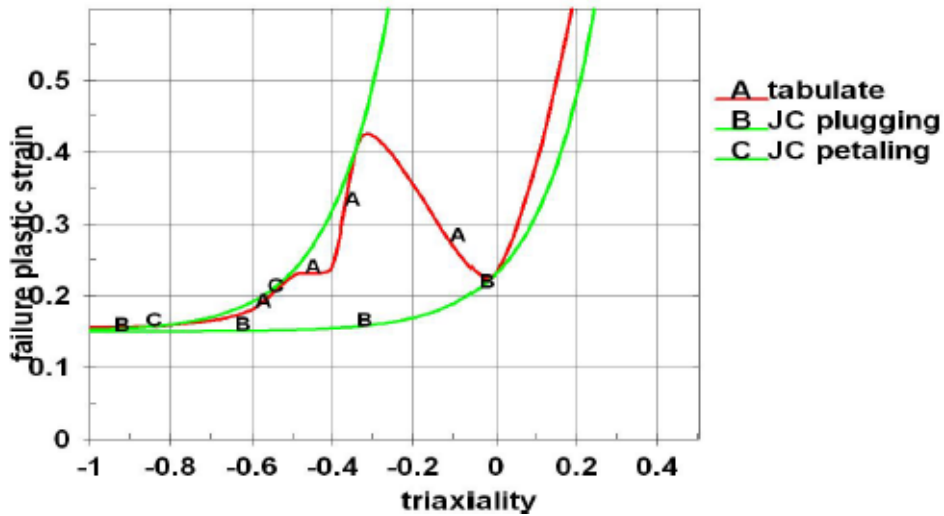
Fig.3: *Comparison of analytical MAT_15 (J-C) and tabulated MAT_224 capability of defining failure plastic strain versus triaxiality.*

The development of MAT_224 was closely based on J-C MAT_15 with the same multiplicative decomposition approach for both yield stress and failure strain, except that the analytical formulations for the stress-strain relationship defining the flow stress and failure strain dependence on strain rate and temperature are replaced by tabulated data. The flow stress is defined by a table of rate-dependent isothermal hardening curves and a table of temperature-dependent quasistatic hardening curves. Similarly, the plastic failure strain is defined by a table of load curves giving plastic failure strain over triaxiality, σ^*, for each Lode parameter, θ_L, expressed in equation (6) as *f*(), plastic strain rate, $\dot{\varepsilon}_p$, scaling expressed as *g*(), and temperature, *T*, scaling expressed as h(), as well as element size, l_c (square root of element area for shells and volume over maximum area for solids), regularization expressed as *i*() by

$$\varepsilon_{pf} = f(\sigma^*, \theta_L) g(\dot{\varepsilon}_p) h(T) i(l_c) \tag{6}$$

Additional capabilities including optional coupling with equation of state, *E* modulus as a function of temperature, and ability to specify the Taylor-Quinney coefficient as a function of strain rate, as well as logarithmic interpolation for rate scaling were subsequently implemented as driven by demand from industrial users. Further, the failure strain regularization was also recently made a function Lode parameter, as well as triaxiality.

The development of MAT_224 required an extensive experimental test program for material characterization as well as intense numerical development. The Ohio State University (OSU)

conducted the experimental portion, and George Washington University (GWU) was responsible for computational model development. NASA-GRC conducted ballistic impact tests to be used for validation on this effort. Aluminum 2024-T351 was chosen as the first candidate material because of its wide use in aerospace structural applications. To minimize model error from plate to plate material differences, all of the characterization tests were performed from a single 0.5″ thick plate. Tests were run to characterize the plastic deformation and ductile fracture behavior. The specimen geometries and loadings were chosen to cover as many applicable states of stress as possible over a broad range of strain rates ranging from $10^{-4} \, s^{-1} - 11,000 \, s^{-1}$ and temperatures ranging from 50º–450ºC. The process has been documented in a series of publicly available FAA reports [4, 5, 6]. Extensive validation efforts are underway and have illustrated the need for additional testing to resolve simultaneous full-field strain and temperature measurements as discussed in later sections.
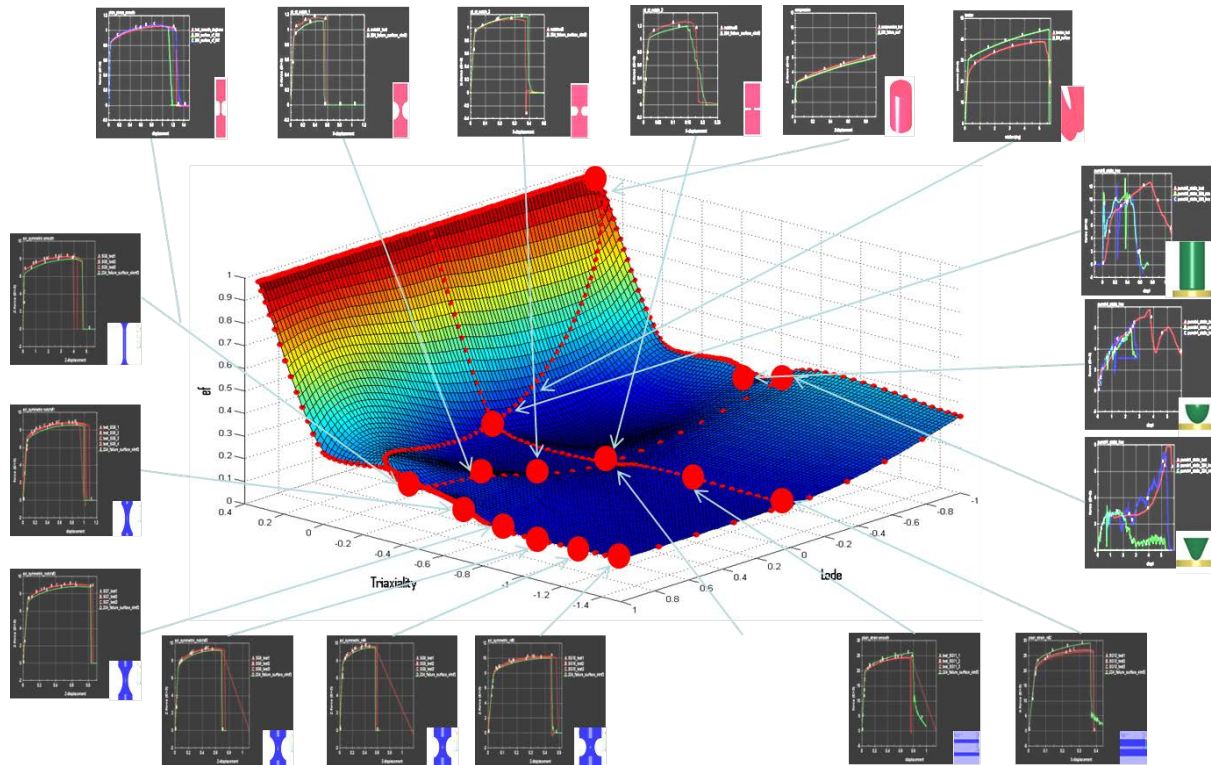
Fig.4: Failure surface for MAT_224 Al 2024 illustrating the different material characterization tests used to obtain plastic failure strain for different states of stress defined by triaxiality and Lode.

3.3 Development of MAT_224_GYS *MAT_TABULATED_JOHNSON_COOK_GYS

During experimental characterization testing of the next material Ti-6Al-4V at OSU, it became apparent that the material displayed an asymmetry in tensile and compressive yield, and it was determined that a model based on J_2 plasticity could not precisely capture the plastic response observed in both tension and compression loading. Therefore, development of a material model with a J_3 (third deviatoric stress invariant) dependent yield surface began at GWU.

The MAT_224 tabulated Johnson-Cook model uses classical J_2 (von Mises) plasticity and is well suited for use with materials in which the yielding in tension and compression are the same and the shear yield is $1/\sqrt{3}$ of that in tension. A stress-state-dependent generalized yield surface (GYS) is necessary to capture a material response that exhibits a yield strength differential in tension and compression or a shear yield that does not conform to J_2 plasticity. Metals such as magnesium and titanium alloys have a hexagonal close-packed (HCP) crystal structure and are known to exhibit a stronger strength differential in yield due to differing dominant plastic deformation mechanisms than face-centered cubic (FCC), such as aluminum, or body-centered cubic (BCC) metals, such as steel.

The GYS model proposed would be an extension of MAT_224 with all the same essential features, namely, an isotropic material law available for solid elements that follows a tabulated approach. Therefore, MAT_224_GYS also has strain rate and temperature sensitivity, element regularization, and a failure surface defining plastic failure strain versus triaxiality and Lode parameter. The yield function is defined

$$f\left(\sigma_{eff}, \sigma_y\right) = \sigma_{vm}\left[c_1 + c_2\theta_L + c_3\theta_L\right] - \sigma_y \tag{7}$$

The user defines additional rate- and temperature-dependent curves giving the compressive and shear yield stresses as a function of plastic strain, plastic strain rate, and temperature.

As shown in figure 4, both MAT_224 and MAT_224_GYS match the uniaxial tension force-displacement data well at a strain rate of $1s^{-1}$ at room temperature. However, only MAT_224_GYS and not MAT_224 can also match the compression test data when a strength differential is exhibited, as shown in figure 5. In this case, the MAT_224 output in compression underestimates the compression. The consideration of yield strength differential results in difference in failure prediction between MAT_224 and MAT_224_GYS, as shown in figure 6. Single-element tests using the same failure surface and contrived strength differentials were used to illustrate this effect. Even though the plastic strain to failure used was the same for both models, the path to failure is different because of the strength-differential effect. An FAA report will be produced providing details on the numerical development of MAT_224_GYS.
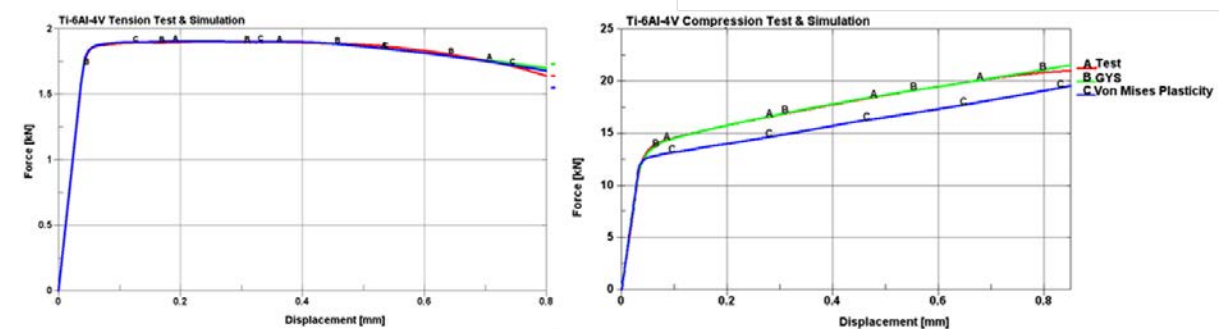
Fig.5: *Comparison of tension (left) and compression (right) tests using MAT_224_GYS and MAT_224 to experiments conducted at OSU. All specimens were cut from the same 0.5" thick Ti-6Al-4V plate.*
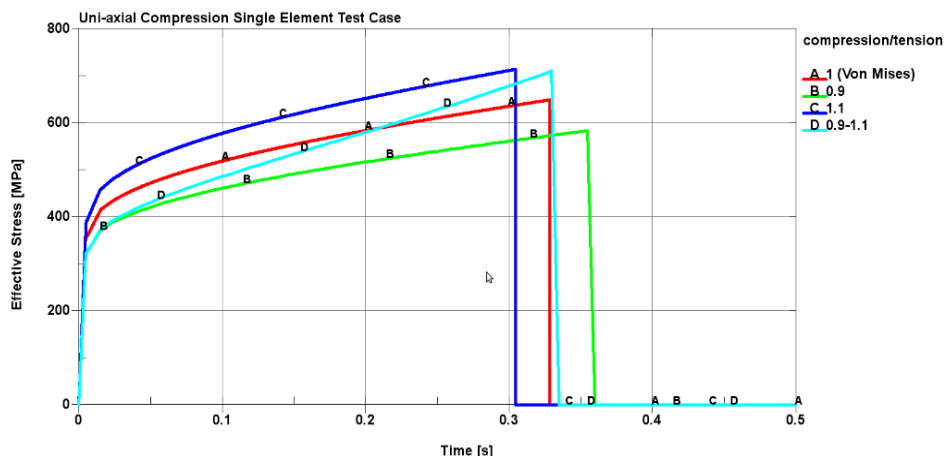
Fig.6: *Effect of the uniaxial compression/tension yield ratio on failure in a single element uniaxial compression simulation.*

3.4 Development of MAT_264 *MAT_TABULATED_JOHNSON_COOK_ORTHO_PLASTICITY

It also became apparent during testing at OSU of Ti-6Al-4V that, while the 0.5″ thickness plate was relatively isotropic, the 0.25″ plate exhibited significant anisotropic effects (figure 7). Although many

anisotropic material models exist in LS-DYNA, they are intended primarily for metal forming applications and do not have all the essential ingredients necessary for simulating impact, as shown in table 1.

	Material Model Number and Description	Strain Rate	Failure	Thermal	Anisotropic	Damage	Asymmetric
033	Barlat Anisotropic Plasticity (YLD96)	Y			Y		
036	Three-Parameter Barlat Plasticity	Y		Y	Y		
133	Barlat YLD2000	Y		Y	Y		
135	Weak and Strong Textured Model	Y	Y		Y		
224	Tabulated Johnson-Cook	Y	Y	Y		Y	
224_GYS	Tabulated Johnson-Cook Generalized Yield Surface	Y	Y	Y		Y	Y
233	Cazacu Barlat				Y		Y
243	Hill 90	Y		Y	Y		
264	Tabulated Johnson-Cook Orthotropic Plasticity (Available in R.10)	Y	Y	Y	Y	Y	Y

Table 1: Available plasticity models in LS-DYNA

Therefore, the team consisting of George Mason University (GMU), OSU, Livermore Software Technology Corporation, NASA-GRC, and the FAA set about developing a suitable anisotropic model capable of considering an orthotropic elastic plastic material law in addition to a strength differential in tension and compression. The effort has been documented in an FAA report [7]. MAT_264 is built upon the features of the isotropic model MAT_224_GYS extending them to account for directional dependence of the material law while incorporating the necessary strain rate and temperature dependency. MAT_264 includes tabulated input for the rolling direction, identified as 0 degrees and also data for 45 degrees, 90 degrees and through the thickness (tt). This is the only anisotropic available in LS-DYNA that has the capability of modeling a directional and tabulated tension/compression yield asymmetry. As with MAT_224 and MAT_224_GYS, it is implemented for fully solid elements necessary for impact applications. Initial impact simulations of the Ti-6Al-4V appear promising, as shown in figure 8 illustrating the stress directionality obtained using MAT_264. MAT_264 is being incorporated into LS-DYNA and will be available in the next full release.
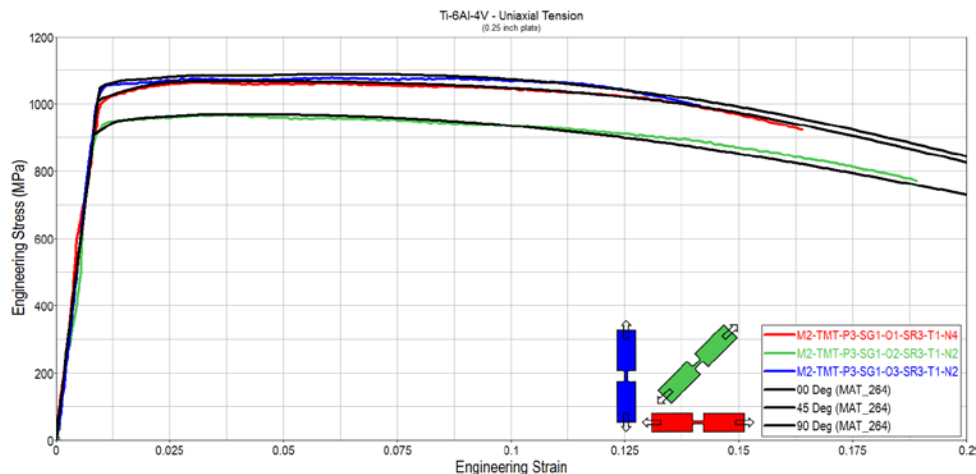
Fig.7:   Anisotropic material response of a 0.25" Aluminum-2024 plate in uniaxial tension. The MAT_264 anisotropic material model (black curves) is able to accurately match the experimental data for all directions.
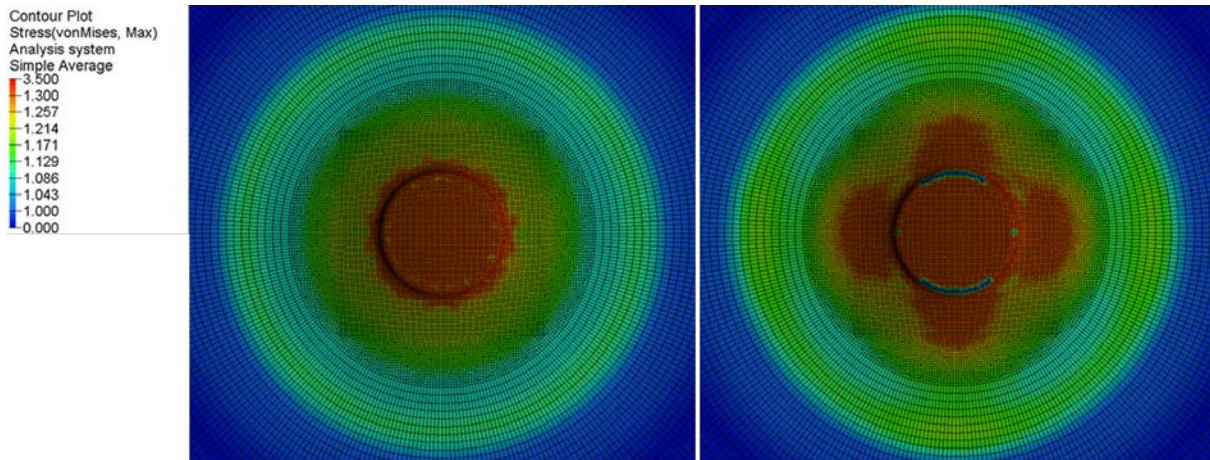
Fig.8:   Comparison of von Mises stress distribution between isotropic MAT_224 (left) and anisotropic MAT_264 (right) of a 0.25" Ti-6Al-4V plate impacted by a cylindrical projectile at 751 ft/s. The anisotropic model shows a clear stress directionality with comparatively less stress in the 45-degree direction when compared with the 0- and 90-degree directions.

3.5   Material Features and Metals Characterized

The model features for MAT_224, MAT_224_GYS, and MAT_264 are summarized in table 2. In addition, the metals characterized for use with each model are also noted. The availability of models that are capable of resolving more complex material response gives the analyst the ability to start simple and choose a more advanced model when necessary. Therefore, we begin with MAT_224 and turn to MAT_224_GYS and MAT_264 when strength differential or anisotropic properties are demonstrated by testing. The original aluminum rev0 2024 MAT_224 material model was the first material characterized and full-field strain data from Digital Image Correlation (DIC) at high strain rates was not available. In subsequent material characterization efforts for Ti-6Al-4V, full-field strain data has proven critical in generating accurate strain rate and temperature-dependent hardening curves. As a result, OSU is now conducting new tests to obtain DIC data for aluminum 2024, which will result in a better material characterization, denoted as aluminum 2024 rev 1 in table 2. Similar efforts are also in progress for 0.25″ Ti-6Al-4V requiring strain rate and temperature testing in additional orientations. Stainless steel 410 is the next material which will be characterized beginning with MAT_224.

	MAT_224	**MAT_224_GYS**	**MAT_264**
Element type	Solid/Shell	Solid	Solid
Degree of yield anisotropy	Isotropic	Isotropic	Orthotropic
Yield DoF	1: Tension 00	3: Tension 00 Compression 00 Shear 00	9: Tension/Compression 00/45/90/tt Shear 00
Flow DoF	0: Associated	0: Associated	0: Associated
Strain rate effect	Yes	Yes	Yes
Temperature effect	Yes	Yes	Yes
Asymmetric yield	No	Yes	Yes

Tabulated distortional work hardening	N/A	Yes	Yes
Imposed convexity	N/A	Yes	Partial
Metals Characterized			
Completed	Aluminum 2024 Rev0 Ti-6Al-4V 0.5" Rev0 Inconel 718 Rev0		Ti-6Al-4V 0.25" Rev0
Ongoing	Aluminum 2024 Rev1	Ti-6Al-4V 0.25" Rev0	Ti-6Al-4V 0.25" Rev1
Future	Stainless Steel 410	TBD	TBD

Table 2: Available tabulated material model features and metals characterized with FAA support.

4 Discussion

4.1 Challenges

4.1.1 Sparse areas of failure surface

Important areas of the failure surface along the Lode=-1 meridian remain underpopulated with experimental data. Ballistic impact simulations show that failure can occur in the regions defined by these states of stress. However, current experimental specimen tests used to generate the surface do not offer multiple data points in an area covering these stress states. Novel punch tests are being designed by OSU with the aid of LS-DYNA simulations to target a specific state of stress region based on adaptions of the standard ASTM quasi-static hemispherical punch tests. The goal is to create additional experimental designs that can be utilized to provided additional plastic failure strain data along the Lode=-1 curve between a triaxiality of -2/3 and 1/3. This work was detailed in a paper presented at the 14th International LS-DYNA Users Conference [8].

The team recognized that states of stress along the Lode=-1 meridian could be interpreted as a combination of in-plane equi-biaxial tension and out-of-plane compression defined as

$$\sigma = \begin{bmatrix} 1 & 0 & 0 \\ 0 & 1 & 0 \\ 0 & 0 & b \end{bmatrix} \sigma_{xx} \tag{8}$$

The relative contribution of either the in-plane tension or out-of-plane compression could be tuned through the dimensionless parameter *b* defined as

$$b \equiv \frac{\sigma_{zz}}{\sigma_{xx}} \leq 0 \tag{9}$$

By varying *b* from 0 (equi-biaxial plane stress tension) to $-\infty$ (uniaxial compression out-of-plane), the triaxiality can range from -2/3 to 1/3 with Lode parameter held constant at -1. LS-DYNA was used to perform simulations to help design the experiment to ensure that the correct triaxiality and Lode parameter were obtained and maintained during damage accumulation all the way up to failure. It was determined from the simulations that a very small punch diameter (2.25-mm punch in a 51-mm-diameter clamp + die) would be necessary to induce failure at the center point of maximum displacement on the backside of the 1.27-mm-thick Al-2024 specimen and to minimize influence of the die/clamp boundary conditions. The simulations showed that this setup encourages failure at the position on the specimen which achieves a nearly constant triaxiality of approximately -0.64 with Lode=-1 up to the point of failure as desired.

To increase the influence of out-of-plane compression relative to in-plane biaxial tension, an annealed copper backing plate was used behind the specimen in the punch setup. This setup used the same punch diameter of 2.25 mm but with a 25.4-mm diameter hole. The specimen thickness stayed at

1.27 mm and the Cu backing plate was also 1.27-mm thick. Simulation results show that this setup maintains a relatively stable triaxialility of -0.53 in the first element to erode up to the point of failure. Annealed copper was used because it is both more ductile and lower strength than the 2024 aluminum encouraging the specimen to fail before the backer plate and in the center on the back side of the specimen. It is conceived than in the limit of a zero-strength backing plate, the specimen stress state tends toward pure equibiaxial tension (Lode=-1, triaxiality =-2/3), and in the limit of a rigid back plate, the specimen stress state tends toward pure out-of-plane compression (Lode=-1, triaxiality=1/3). First experiments using these novel designs are currently underway. If successful, additional tests will be designed to further explore regions of increasing triaxiality along the Lode=-1 curve.

4.1.2 Coupled strain rate and temperature effects

The strain rate and temperature influence can have a profound effect on the deformation and failure response of a material. Therefore, accurate experimental characterization tests are necessary at elevated strain rates and temperatures. High strain-rate tests are accomplished with a variety of Split Hopkinson Bar (SHB) setups that load the specimens in tension, compression, or torsion. Very small samples are an experimental necessity at high strain rates. DIC has proven indispensable in testing because the strain fields will inevitably deviate from the desired uniform distribution during localization. With the use of DIC, the strain fields obtained in the LS-DYNA simulated specimen tests can then be closely correlated with the experiments.

High strain rates and elevated temperatures typically have opposite effects on the flow response of the material. An increase in strain rate is often associated with plastic hardening, whereas an increase in temperature results in thermal softening. However, at high strain rates, there is not enough time for significant heat transfer to occur, and a strongly localized increase in temperature due to the plastic work is realized. Therefore, the strain rate and temperature response are coupled. OSU recently developed a new experimental setup in which full-field temperature can be measured simultaneously with full-field DIC. The visual cameras image one side of the specimen while a high-speed infra-red camera measures the radiated temperature on the other side. Tests can be accomplished over a very broad range of strain rates from $10^{-4} s^{-1} - 3000 s^{-1}$. The very high frame rate thermal cameras are essential for capturing accurate peak temperature measurements at high strain rates. New tests using this setup will help isolate the strain rate and temperature effects which will considerably facilitate the generation of numerical models from experimental data.

4.1.3 Material property variation

To have truly predictive simulations that can match the observed ballistic impact test results, ideally an extensive material testing program should be carried out to characterize the deformation and failure response of the material as comprehensively as possible. However, practically these tests are expensive and time consuming. Manufacturing various thickness plates and sheets of a given metal alloy can often introduce within specification variability. The metallic microstructure can be affected by differences in the chemistry, metal working process, and heat treatment which can change the mechanical properties of the material affecting the failure response. It should be noted that plate thickness is only one of the factors that can influence the mechanical properties, and variations between batches of a given thickness can also have an effect.

Ballistic testing was performed on four Ti-6Al-4V plates of 0.5″, 0.25″, 0.14″, and 0.09″ thicknesses, all with the same temper and meeting AMS-4911 specification. Actual tensile testing results showed that there was a difference in yield stress and failure strain between the different plate thicknesses, although all plates met minimum specification. It is desirable to find a simple way to utilize the material model developed based on plate sample in the simulation of another thickness in an effort to avoid treating each thickness as essentially a separate material, which would necessitate a full suite of testing for each thickness/manufacturing thickness.

4.2   Lessons Learned

The metallic material characterization and failure model development effort funded by the FAA ACFPP has developed a suite of new analytical modeling capabilities in LS-DYNA. These models offer the analyst exciting new capabilities that are improving model accuracy. These models require meticulous modeling of experiments in the development of the model. As the teams of researchers have been met with challenges, increases in testing capability have provided insight into the nuances. Processing

speeds and memory have provided the backbone of the advances in testing and analysis, enabling the practical use of a fine finite element mesh.

A robust experimentally data-driven approach is necessary to derive the material characterization and validation test data. If possible, the material characterization specimens and ballistic impact validation test material should come from an identical sample and the simulation mesh sizes in material characterization and validation tests should be comparable because mesh regularization has its limits. Differences in material processing, especially in HCP metals can affect material properties which influence the impact response of different thickness plates or sheets for a given chemistry even with all meeting the same AMS specification. Even property variation from batch to batch for a given thickness may have an effect and therefore the manufacturing process should be tightly controlled for critical applications.

Close cooperation between the modeler and test lab is essential. The test data should be delivered in a consistent and mutually accepted format to minimize communication errors and the force-displacement data should be synchronized with the strain field data (if available). Full-field strain measurement from DIC has become an extremely useful tool for accurate material characterization. This technique was introduced in the middle of the testing program at OSU for 2024 aluminum rev0 for the initial MAT_224 model development and was used subsequently for the titanium and Inconel testing. The DIC data has allowed the full strain field to be matched precisely between test and simulation, as show in figure 9. The DIC pattern should cover as much of the specimen as possible, not just the gage section, so that boundary conditions are accurately captured. It can be stated safely that a material model capable of matching the full strain field is a necessary condition for a failure model with predictive capability.

DIC is particularly useful at high strain rates when local strain rates within the specimen gage section can far exceed the nominal applied strain rate. Additional testing using DIC for the aluminum 2024 rev1 is currently being conducted at OSU and will also include high-rate testing with simultaneous temperature measurements. Thermal measurements made during material characterization tests conducted at OSU have shown that a significant temperature increase can occur at strain rates as low or lower than $1\,s^{-1}$ previously thought to be effectively isothermal. The "quasi-static" baseline curves need to be close to isothermal, and this may necessitate going to extremely low strain rates.

Fig.9: Comparison of strain fields from DIC experiment and simulation for uniaxial tension.

The tabulated nature of the stress-strain curves and failure surface can create unphysical behavior from LS-DYNA extrapolation if the user does not take appropriate care. This is particularly true in bounding the failure surface because it became apparent that LS-DYNA was extrapolating the tensile triaxiality region to very low plastic failure strain values beyond the data points that were populated from testing. A plateau was added to correct this issue to prevent extrapolation to unrealistically low plastic failure strain values. Such an issue is not present with the MAT_15 model because the curves become horizontally asymptotic at high tensile triaxiality. This also underscores the need for good engineering judgement in constructing the failure surface, because simulations will undoubtedly encounter stress states in some elements that are not near experimental data points.

The generation of the failure surface is an iterative process due to experimental limitations in exercising complex states of stress that leave areas of the surface sparsely populated. To some degree, the modeler must utilize a trial and error process of modifying the surface to match the simulation results with those actually realized in tests. Obtaining the correct ballistic curve is insufficient if the simulation does not physically resemble the impact test failure mode. Therefore, the plastic failure strain on a portion of the surface may need to be adjusted to get a physically realistic simulation that correlates well with tests over many cases. LS-OPT may be well suited in standardizing a method for constructing the failure surface.

Because all experiments involving ductile methods exhibit localization of plastic deformation, the load paths are non-proportional even for simple sample shapes, and matching test results accurately can only be achieved by a reverse-engineering process.

4.3 Ongoing Work

4.3.1 Ballistic Validation

Experimental ballistic impact tests of spherical projectile shapes impacting different thickness flat panels at a normal angle of incidence are crucial validation points to match simulation results against and assess the predictive fidelity of the model. These tests can be well controlled as the projectile geometry presented to the target plate is not affected by the sphere's orientation. The FAA ACFPP-funded ballistic impact testing of aluminum 2024 targets of 0.063″, 0.125″, and 0.25″ with 0.5″ diameter steel spheres up to velocities of 900 ft/s at UCB [1]. The testing produced ballistic velocity curves as shown in figure 2 and the reliability of the new material models is assessed in large part by how accurately they can match with these tests. Matching the correct failure mode and the ballistic curve is also necessary.

A significant challenge in developing and validating the accuracy of predictive impact models can occur when the material characterization data used to generate the computational model input decks is obtained from a different source than the ballistic impact validation. Care has been taken under this effort to use identical material stock to manufacture the material characterization specimens as well in fabricating the ballistic impact test panels. As detailed in [10], panel tests were conducted at NASA-GRC for aluminum 2024 panels of thickness 0.125″, 0.25″, and 0.5″ and also Ti-6Al-4V panels of thickness 0.09″, 0.14″, 0.25″, and 0.5″. Small panel (15″ x 15″) tests were conducted with cylindrical projectiles at normal incidence. Validation results so far using MAT_224 for the 0.5″ Ti-6Al-4V show a good correlation between simulation and test, as shown in figure 10. Similar testing efforts are underway for Inconel 718 plates and stainless steel 410 plates to provide data to validate the material models against.
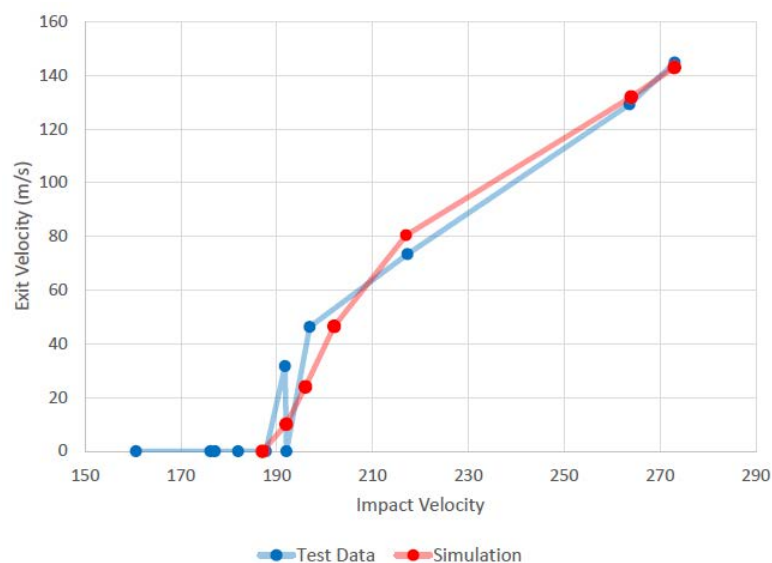
Fig.10: Ballistic impact test validation for MAT_224 0.5″ Ti-6Al-4V [11].

4.3.2 Further Material Characterization

Stainless steel 410 will be the next metal material model characterized. The rate- and temperature-dependent strain-hardening tables will first be developed for MAT_224 based on experimental data. The failure surface will then be developed by carefully matching simulations to tests data. The material model will then be evaluated against ballistic test data. If strength differential and anisotropic effects preclude the effective use of MAT_224, then MAT_224_GYS or MAT_264 will be used. The effort will be documented in publicly available FAA reports. Additional future efforts will be focused on development of material models for composite materials.

4.3.3 Variable Taylor-Quinney Coefficient

During an impact event, heating occurs due to conversion of plastic work. The temperature increase from adiabatic heating due to plastic work can be expressed as

$$T = T_R + \frac{\beta}{c_p \rho} \int_0^{\varepsilon_p} \sigma_y \dot{\varepsilon}_p dt \qquad (15)$$

where T_R is the ambient temperature, c_p is the specific heat at constant pressure, ρ is the density, σ_y is the yield stress, $\dot{\varepsilon}_p$ is the plastic strain rate, and β is the Taylor-Quinney coefficient representing the fraction of plastic work converted to heat. The assumption of adiabatic heating at high strain rates is well justified at high strain rates in which there is little time for significant heat transfer to occur within the specimen and to the surroundings. However, at lower strain rates, the process cannot be considered adiabatic. As detailed in [5], several experiments have found that the amount of work converted to heat could vary widely depending in the strain or strain rate for certain metals. MAT_224, MAT_224_GYS, and MAT_264 all have the ability to specify a variable Taylor-Quinney coefficient. The coupled strain and temperature measurement testing currently being accomplished at OSU will aid in determining the dependence of β on strain and strain rate. The variable Taylor-Quinney coefficient can be used to model the physical dependency of the energy conversion upon strain, strain rate, and temperature as wel as to compensate for head conduction in purely mechanical analyses.

4.3.4 Further Model Development–Anisotropic Failure

Experimental testing has shown that the out-of-plane shear failure strain is quite different from the in-plane failure strain. In its current incarnation, MAT_264 only allows for orthotropic yield, but the failure is isotropic. Existing options in LS-DYNA such as *MAT_ADD_GENERALIZED_DAMAGE hold promise for accomplishing this task, but must be extended to truly 3-D states of stress to include failure dependent on Lode parameter and triaxiality.

5 Summary

The FAA has sponsored multi-year research for developing computational models for simulating fan blade-off containment and engine-related impact events. Truly predictive models that can accurately replicate the transition from petaling to plugging failure modes of metals without tuning the model to match specific tests is essential for acceptable certification by analysis. These efforts have resulted in the implementation of new tabulated J-C-based plasticity models MAT_224, MAT_224_GYS, and MAT_264 in LS-DYNA. An extensive experimental material characterization is in progress to create material models for several aerospace metals. The development of the triaxiality and Lode-parameter-dependent failure surface is met with several challenges, including sparse areas which require the development of novel tests and accurately capturing and modeling strain rate and temperature effects. Although continued model development is planned, efforts in the near future will focus on rigorous validation against ballistic tests to assess the reliability of the models. The FAA effort is directed towards establishing a methodology rather than making models available to industry. It is emphasized that material characterization will still need to be performed according to the FAA guidelines for particular applications and materials.

6 Literature

[1] Kelley, S. and Johnson, G.: "Statistical testing of aircraft materials for transport airplane rotor burst fragment shielding," DOT/FAA/AR-06/9, 2006.

[2] Buyuk, M., Loikkanen, M., and Kan, C.-D.: "Explicit finite element analysis of 2024-T3/T351 aluminum material under impact loading for airplane engine containment and fragment shielding," DOT/FAA/AR-08/36, 2008.

[3] Liang R. and Khan A.S.: "A critical review of experimental results and constitutive models for BCC and FCC metals over a wide range of strain rates and temperatures," International Journal of Plasticity, vol. 15, 1999, 963–980.

[4] Emmerling, W., Altobelli, D., Carney, K., and Pereira M.: "Development of a new metal material model in LS-DYNA Part 1: FAA, NASA, and industry collaboration background," DOT/FAA/TC-13/25 P1, 2014.

[5] Buyuk, M.: "Development of a new metal material model in LS-DYNA Part 2: Development of a tabulated thermo-viscoplastic material model with regularized failure for dynamic ductile failure prediction of structures under impact loading," DOT/FAA/TC-13/25 P2, 2014.

[6] Seidt, J. D.: "Development of a new metal material model in LS-DYNA Part 3: Plastic deformation and ductile fracture of 2024 aluminum under various loading conditions," DOT/FAA/TC-13/25 P3, 2014.

[7] Haight, S. H.: "An anisotropic and asymmetric model for simulation of metals under dynamic loading," DOT/FAA/TC-TT16/44 2016.

[8] Lowe, R. L., Seidt, J. D., and Gilat, A.: "Characterization of the Lode=-1 meridian on the Al-2024 failure surface for *MAT_224 in LS-DYNA," 14th International LS-DYNA Users Conference, 2016.

[9] Wang, L., Dicecca, F., Haight, S., Carney, K. DuBois, P., Emmerling, W., and Kan, C.-D.: "Test and simulation comparison using titanium material models based on MAT_224," 14th International LS-DYNA Users Conference, 2016.

[10] Pereira, M. J., Revilock, D. M., Lerch, B. A., and Ruggeri, C. R.: "Impact testing of aluminum 2024 and titanium 6Al-4V for material model development," DOT/FAA/TC-12/58, 2013.

[11] Haight, S., Wang, L., Du Bois, P., Carney, K., Kan C.-D.: Development of a titanium alloy Ti-6Al-4V material model used in LS-DYNA," DOT/FAA/TC-15/23, 2016.